Optical Materials 31 (2009) 1284–1287

Contents lists available at ScienceDirect

Optical Materials

journal homepage: www.elsevier.com/locate/optmat

Amplification from Nd^{3+} doped Si–Ti sol–gel channel waveguides

Asher Peled [a,*], Menachem Nathan [a], Ady Arie [a], Alexander Tsukernik [b], Shlomo Ruschin [a]

[a] Department of Physical Electronics, Faculty of Engineering, School of Electrical Engineering, Tel Aviv University, Tel Aviv 69978, Israel
[b] The Center for Nanoscience and Nanotechnology, Tel Aviv University, Tel Aviv 69978, Israel

ARTICLE INFO

Article history:
Available online 6 December 2008

PACS:
42.60.Da
42.70.−a
42.82.Gw

Keywords:
Neodymium
Sol–gel waveguide
Amplifier
Grating coupler
Up-conversion

ABSTRACT

We report the sol–gel chemistry reaction system and processes used to realize the first grating coupled monolithic solid state optical amplifier based on a Nd^{3+} doped sol–gel tapered rib waveguide. The sol–gel matrix composition is $50SiO_2$:$50TiO_2$:$10AlO_{1.5}$:$1NdO_{1.5}$. The signal (1064 nm) and pump (803 nm) beams were coupled via grating couplers into and out of the rib waveguide. A photoluminescence lifetime of 138 μs and a pump absorption cross-section of $1.79 \times 10^{-24}\,m^{-2}$ were measured. A net internal gain of 3.75 dB/cm was achieved. Theoretical simulations predict that this gain could be further improved. Analysis of the results suggests that the difference between achieved and predicted gain is due to low quantum efficiency caused by two-ion cross-relaxation and up-conversion, as manifestly evident by yellow light emitted from the device. The molecular-level processes during the doped sol–gel fabrication that could lead to these phenomena are discussed, and strategies are suggested to overcome these limitations in order to approach the full potential gain.

1. Introduction

Integrated optics biosensors are optical waveguide (WG) based devices capable of sensing of a specific bio-molecule analyte. The specificity of these sensors is achieved by fixation of "bio-receptors" such as antibodies to the sensor surface. Once the sensor is exposed to the sample liquid, the target bio-molecules are specifically bound to the bio-receptors on the sensor surface. The bound layer interacts with the evanescent fields of the guided waves and impacts their propagation coefficient. Channel waveguiding enables interferometric detection schemes such as WG-based Mach–Zehnder interferometers (WMZI). Although WMZI biosensors are most sensitive, their use is currently limited to optical lab environments due to their high cost and the need of delicate coupling of light source and detectors to the sensor chip restricts their use to optical lab environments. Recently, we reported the first pure monolithic solid state amplifier [1] realized in a Nd doped sol–gel rib WG. The amplifier was developed as part of an effort to establish a monolithic and integrated sol–gel-based light source for Lab-on-chip applications. The sol–gel method used is fully compatible with silicon technology. The sol–gel precursors are extremely inexpensive, the layers are applied by simple spin-coating on regular silica-on-silicon (SOS) and the fabrication is purely monolithic – no edge polishing or processing is required. In this paper, we present the sol–gel chemistry reaction system and processes used to realize this device and report on the phenomenon of strong up-conversion observed in the device. In addition, we present and analyze the comparison of the measured gain with that predicted by theoretical simulations of the device. The theoretical simulations indicate that the gain can be much improved relative to that measured by using a different host composition. The possible mechanisms responsible for that difference as well as the molecular-level processes of the doped sol–gel components that could lead to this phenomenon during its fabrication are analyzed. We conclude by suggesting different strategies regarding the sol–gel composition and preparation process for avoiding these limitations and for achieving the full potential gain predicted by the theoretical simulations.

2. Experimental

2.1. Nd doped silica–titania sol–gel reaction system and fabrication process

The sol–gel solution was prepared by reflux at 77 °C of the following precursors; γ-glycidoxypropyltrimethoxysilane (GLYMO), titanium ethoxide, acetic acid and ethanol. The titanium-alkoxide precursor is added to reach a higher refractive index for the sol–gel guiding layer relative to that of the silica of the SOS substrate. The chemical reaction system is the following:

* Corresponding author. Tel.: +972 3 6408247; fax: +972 3 6423508.
E-mail address: asherp@eng.tau.ac.il (A. Peled).

0925-3467/$ - see front matter © 2008 Elsevier B.V. All rights reserved.
doi:10.1016/j.optmat.2008.10.038

$$CH_3COOH + C_2H_5OH \rightarrow CH_3COOC_2H_5 + H_2O \quad (1)$$

$$Ti(OEt)_4 + CH_3COOH \rightarrow CH_3COOTi(OEt)_3 + EtOH \quad (2)$$

$$Ti(OEt)_4 + 4H_2O \rightarrow Ti(OH)_4 + 4EtOH \quad (3)$$

$$R - Si(OCH_3)_3 + 3H_2O \rightarrow R - Si(OH)_3 + 3CH_3O \quad (4)$$

$$nTi(OH)_4 + nSi(OH)_4 \rightarrow Ti_nO_{2n} + Si_nO_{2n} + 4nH_2O \quad (5)$$

Polymers formed with low water content are better suited for layer formation, using either spin-coating or dip coating [1,2]. Low water concentration prevents TiO_2 dissolution and aggregation of large TiO_2 colloids that cause optical scattering [3,4]. It also prevents uncontrolled gelling. On the other hand, in order to form a cross-linked SiO_2–TiO_2 siloxen network in a 3D structure, 2 moles of water are needed per mole of metal. A smaller molar fraction of water leads to chain polymer formation. Therefore the water content should be tightly balanced and controlled during the sol–gel process. For this reason, water is excluded from the precursors. The water required for the hydrolysis of titanium-ethoxide and GLYMO Eqs. (3) and (4), is formed in the esterification of the acetic acid and the ethanol Eq. (1) [5]. Once the water is formed, it is immediately consumed in the hydrolysis reactions and does not reach a concentration that would cause gelling and dissolution of titania colloids. The hydrolysis rate of titanium-ethoxide is also regulated by the availability of titanium-ethoxide, which is lowered by reacting with the acetic acid to form the titanium-acetate complex, and therefore suppresses the formation of the titania colloids. After 2 h of reflux, neodymium–nitrate–hexahydrate and aluminum–nitrate–nonahydrate were dissolved in ethanol and mixed with the solution. The guiding layer was fabricated by 4 cycles of spin-coating at 2000 rpm on a 25 × 25 mm SOS substrate, followed by curing at 100 °C on a hot plate. The chip was then annealed at 800 °C for 1 h to remove residual organic groups and solvents, thus achieving the Nd–Al co-doped sol–gel silica–titania network with a molar ratio $50SiO_2$:$50TiO_2$:$10AlO_{1.5}$:$1NdO_{1.5}$.

2.2. Device structure and design

The channel WG has a rib cross-section. The rib (local) width is defined by the lateral distance between two 35 nm deep trenches etched into the guiding layer (Fig. 1). The rib WG starts with a 50 μm wide section that contains an input grating and tapers linearly within 7 mm to a width of 6 μm. This linear tapering is twice as long as the minimal length for adiabatic transition for the pump and signal modal fields [6]. The 6 μm wide section is 3 mm long, and includes an output grating at its end. The grating couplers were calculated and designed using an accurate perturbation analysis [7]. To achieve a single diffraction order (i.e., one order into the WG and an unavoidable one into the substrate), the input angle of incidence for the pump (λ = 800 nm) was designed to be −10°, which implies a grating period of 450 nm and an input angle of −53.4° for the signal (λ = 1064 nm). The grating depth was designed to be 120 nm to achieve a coupling interaction length that corresponds to a waist of 76 μm for the pump beam, which also suits well the mode lateral profile of the 50 μm wide WG. The output grating period was designed to be 470 nm to achieve an output angle of −45°. The input and output grating designed lengths were 157.5 μm and 150.4 μm, respectively, to fairly cover the coupling interaction lengths.

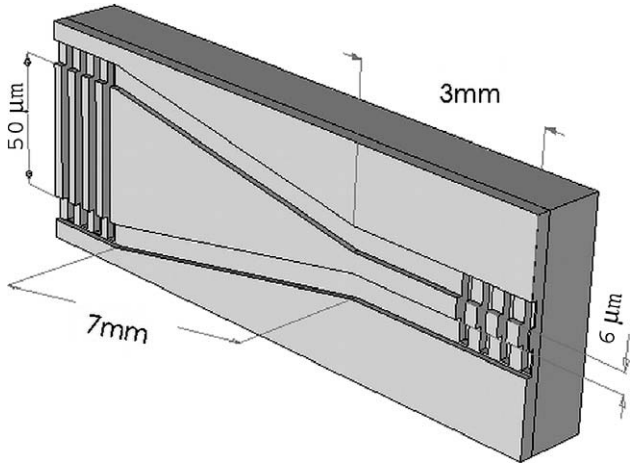

Fig. 1. Amplifier 3D scheme.

2.3. Device fabrication process

The rib WG was defined by ZEP-mediated electron beam lithography (Raith 150) followed by CHF_3 Reactive Ion Etching (RIE) of two 9 μm wide trenches with 35 μm depth. After the WG fabrication, a second lithography and etching process was performed to fabricate the gratings. An additional set of three un-tapered 50 μm-wide devices was fabricated with identical input/output gratings but different lengths: 1 mm, 5 mm and 10 mm. This set was used for attenuation measurements. A similar set was fabricated for pump absorption measurements with an output grating period of 346 nm designed to couple the pump to −45°. A tapered WG with such an output grating was fabricated as well.

2.4. Measurement methods and setups

The sol–gel layer was measured using a spectroscopic ellipsometer (Wollam M2000DUV). The topography of the gratings and the rib was measured in an atomic force microscope – AFM (Di3000 Veeco). A tunable Ti-Sa laser (Coherent 890) was used for pumping and an Nd:YVO laser (λ = 1064 nm) was used as the signal source. The pump and signal beams were focused on the input grating (from two different angles) by 50 mm focal length lenses. The output signal was high-pass filtered (Schott RG 1000) to block the pump light (−41 dB at λ = 803 nm) and measured with a powermeter (Nova Ophir). For attenuation measurements, the signal coupling into the different WGs was optimized in terms of maximizing the power emanating from the output gratings by fine-positioning of the input beam waist on the input grating and by scanning the input angles in the region of −53.4°. Lifetime measurements were performed on a separate setup using an external acousto-optic modulator (NEC OD-88134) and a detector backed with a self-made trans-impedance amplifier connected to a digital scope (Tektronix TDS 2014). The modulated pump beam was prism-coupled to the planar WG and the detector was attached to the WG via the high-pass filter (Schott RG 1000) to suppress the pump light.

3. Results and discussion

3.1. Characterization of geometry and index

The refraction index of the sol–gel film was measured to be 1.814 at λ = 808 nm and evaluated to be 1.803 at λ = 1064 nm. Its thickness was 360 nm. The index at λ = 1064 nm was extrapolated using the Cauchy formula fitted to the data measured at 400 wavelength points, since the measurement was limited to λ = 990 nm due to the ellipsometer. Fig. 2 shows an AFM topographic scan of the output grating at the end of the 6 μm wide section of the rib WG. The grating teeth can be seen on the 6 μm wide rib WG located between the two 9 μm wide trenches. The grating teeth can also be seen at the edge of the AFM scan on the left, as they were written and etched few microns beyond the rib WG trenches.

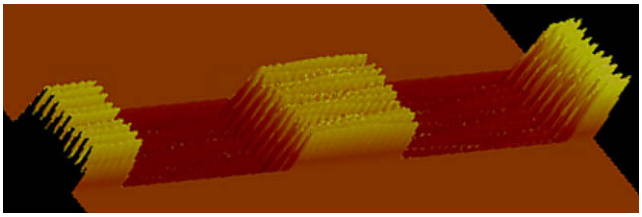

Fig. 2. AFM topographic scan of the output grating coupler at the 6 μ wide WG end.

A grating depth of 180 nm and rib trench depth of 35 nm were measured.

3.2. Lifetime measurements

Fig. 3 shows the measured photoluminescence lifetime. A pure exponential decay with a time constant of 138 μs is seen for the time period at which the noise is negligible ($t < 200$ μs). No fast decay component is seen. The empirical formula relating the observed lifetime τ_{obs} to the rare earth ion concentration n_0 is

$$\tau_{obs} = \frac{\tau_0}{1 + (n_0/Q)^p} \tag{6}$$

where τ_0 is the lifetime in the limit of zero concentration and Q is the quenching concentration which is typical to the hosting glass composition [8]. For the two-ion cross-relaxation mechanism, which is believed to dominate concentration quenching for Nd^{3+} ions [9], $p \approx 2$. This analysis assumes that the rare earth ions are uniformly dispersed throughout the glass and do not cluster. Nd^{3+} doped Al silica has been reported to follow the same concentration quenching curves as the multi-component ED-2 silicate glass [10], for which, $Q = 3.9 \times 10^{26}\ m^{-3}$ and $\tau_0 = 368$ μs [8]. Substituting the Nd^{3+} doping concentration of the sol–gel $n_0 = 2.7 \times 10^{26}\ m^{-3}$ in Eq. (6) with these values predicts a lifetime of 249 μs, which is almost twice that measured. This significant difference implies a proximity for the Nd^{3+} ions which is greater than their concentration, as in the case of aggregation.

3.3. Pump cross-section and coupling efficiency

The output power at $\lambda = 1064$ nm from the 5 mm and 10 mm long untapered WGs, normalized to that of the 1mm long WG, was respectively 0.954 and 0.91, which reveals an attenuation of 0.45 dB/cm. The output power ratio of the 10 mm long tapered WG to the untapered WGs was −0.6 dB. The transmitted powers through the 803 nm pumped WG set were 0.14, 0.03 and 0.003 for, respectively, 1 mm, 5 mm and 10 mm long WGs. This corresponds to an attenuation coefficient of $\alpha = 385\ m^{-1}$. Theoretically, $\alpha = \Gamma\sigma_p N$, where $\Gamma = 86\%$ is the power-filling-factor in the guiding layer, $N = 2.5 \times 10^{26}\ m^{-3}$ is the Nd concentration and σ_p is the absorption cross-section. Thus, σ_p is found to be $1.79 \times 10^{-24}\ m^{-2}$, which is in good agreement with measurements in other silica hosts [11]. Assuming equal efficiencies for the input and output gratings, the coupling efficiency is about 46% for each grating.

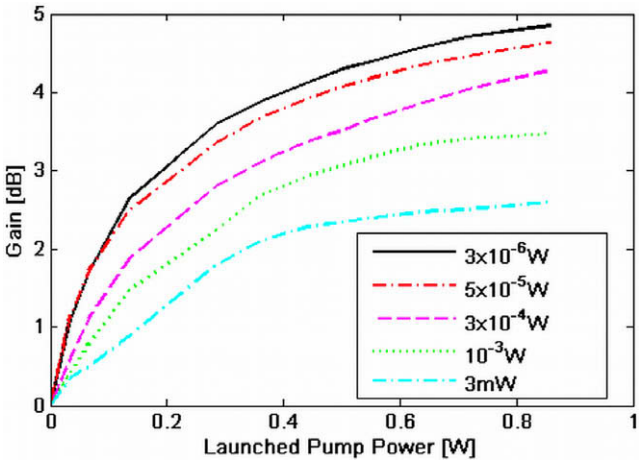

Fig. 4. Gain verses lunched pump power for different signal levels.

3.4. Gain characterization

The photoluminescence (PL) power was measured for the different pump powers, while no signal was launched. The gain was evaluated from the ratio of the output signal power in the presence of pump minus the corresponding PL background, divided by the signal power in the absence of pump. Fig. 4 shows the signal gain as a function of pump power ($\lambda_p = 803$ nm) for five different output signal power levels in the absence of pump. A maximal gain of 4.8 dB (3.75 dB net gain) is seen for an output signal level of 3 μW in the absence of pump. Higher gain was not observed for smaller signal levels. Signal saturation reaches 2.5 dB at a launched pump power of 860 mW and an output signal level in the absence

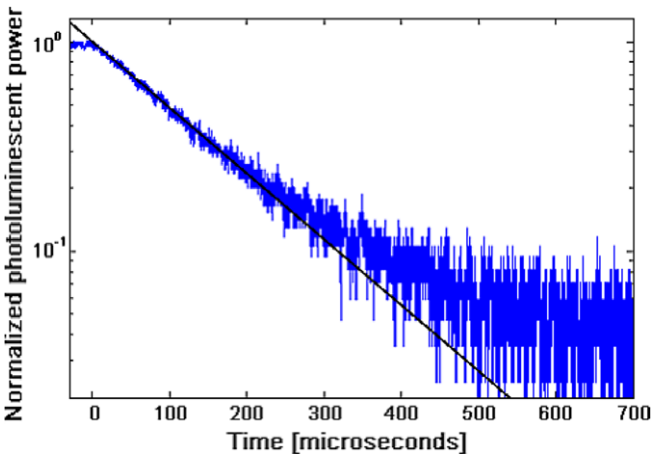

Fig. 3. Photoluminescence lifetime, solid line - exponential fit with 138 μs time constant.

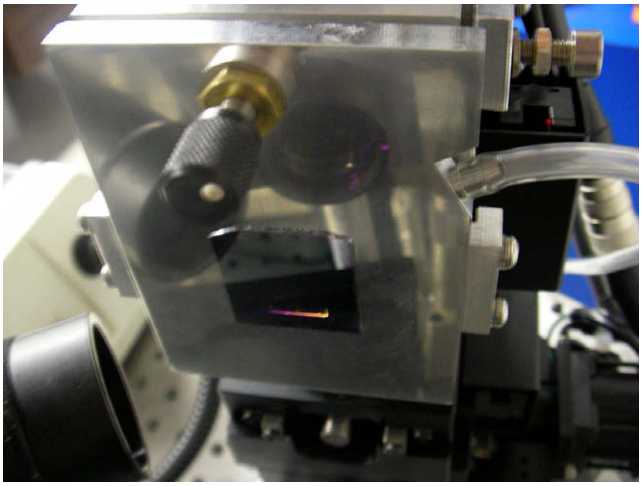

Fig. 5. Optical image of the pumped amplifier, yellow up-conversion light is manifest.

of pump of 3 mW, which corresponds to a saturation output power of about 5.5 mW. Pump saturation is also apparent at the higher pump levels. An up-conversion phenomenon in the device under pumping is seemingly responsible for the saturation as function of pump power. The process is evidenced by a strong yellow light manifested to the naked eye even under ambient lab lighting conditions. Fig. 5 shows an optical image of the amplifier under pumping. The clear yellow light is seen irradiated all along the device, starting at the input grating on the right and ending at the output grating which is 1 cm to the left. The pink color at the yellow line end is due to an artifact of the camera.

4. Discussion

The 3.75 dB net gain measured from the Nd^{3+} doped sol–gel amplifier compares favourably to that of all other Nd^{3+} doped glass channel WG amplifiers [12–16]. Nevertheless, theoretical simulations [17], assuming emission cross-section as reported in [9], predict that the gain can be potentially improved by an order of magnitude. The measured pump absorption cross-section (which agrees with [9]), indicates that the cause for this difference is low quantum efficiency of the amplifier caused by the competing processes – the up-conversion and the two-ion cross-relaxation – rather than inefficient pump absorption. The significant shorter lifetime relative to that predicted by Eq. (6) and the strong up-conversion suggest a proximity of the Nd^{3+} ions which is greater than that expected from their uniform distribution. This proximity could be caused by Al^{3+} ion clustering during the curing of the sol–gel matrix, as well as by the high titanium content, which could lead to titania crystallization. This should be verified in future work. Several approaches could be implemented to prevent Nd^{3+} ions clustering. They include utilizing a rapid thermal annealing for the sol–gel curing and lowering the titanium content in the sol–gel matrix. A more fundamental solution could be achieved by the replacement of the silica–titania matrix with a silica–hafnia sol–gel matrix. A silica–hafnia matrix synthesized by a sol–gel route was recently proven to possess some very good properties as an erbium host glass and as an optical WG [18–21]. The replacement of titanium by hafnium could completely solve the titania crystallization problem as well as the Al^{3+} aggregation problem, since it was shown that the silica–hafnia sol–gel system eliminates the need of Al^{3+} co-doping [22].

5. Conclusions

We report the sol–gel chemistry reaction system and processes used to realize the first monolithic solid state amplifier based on Nd^{3+} doped sol–gel tapered rib WG, for which a net gain of 3.75 dB was achieved from a 1 cm long device. A measured photoluminescence lifetime of 138 μs indicates a certain extent of quenching of the Nd^{3+} ions. We also report an up-conversion phenomenon observed in the pumped device. The thin sol–gel guiding layer used (360 nm) leads to strong evanescent fields, which are ideal for evanescent field sensing. With a net gain of more than 7 dB per round trip, a pure monolithic laser source is achievable by implementing reflection gratings. Such a source could enable fully monolithic optical-based lab-on-chip devices. The comparison of the measured gain with that predicted by theoretical simulations of the device indicates that the gain can be potentially improved by an order of magnitude. Analysis of the results suggests the clustering of Nd^{3+} ions. Several strategies are suggested to overcome these limitations in order to approach the full potential gain predicted by the theoretical simulations.

References

[1] A. Peled, M. Nathan, A. Tsukernik, S. Ruschin, Appl. Phys. Lett. 90 (2007) 161125.
[2] S. Sakka, K. Kamiya, K. Makita, Y. Yamamoto, J. Non-Cryst. Solids 63 (1984) 223.
[3] J.H. Jean, T.A. Ring, Langmuir 2 (1986) 251.
[4] E.A. Barringer, H.K. Bowen, Langmuir 1 (1985) 414.
[5] A. Le'austic, R.E. Riman, J Non-Cryst. Solids 135 (1991) 259.
[6] A.F. Milton, W.K. Burns, IEEE J. Quant. Elect. QE-13 (1977) 828.
[7] T. Tamir, S.T. Peng, Appl. Phys. 14 (1977) 235.
[8] S.E. Stokowski, R.A. Saroyan, M.J. Weber, Lawrence Livermore National Laboratory, M-095, Rev. 2, November, 1981.
[9] Michel J.F. Digonnet, Rare-Earth-Doped Fiber Lasers and Amplifiers, second ed., Marcel Dekker, New York, 2001. Chapter 2, p. 41.
[10] K. Arai et al., J. Appl. Phys. 59 (1986) 3430.
[11] I.M. Thomas, S.A. Payne, G.D. Wilke, J. Non-Cryst. Solids 151 (1992) 183.
[12] U. Aoki, E. Ishikawa, Y. Asahara, Electron. Lett. 27 (1991) 2351.
[13] N.A. Sanford, K.J. Malone, D.R. Larson, R.K. Hickernell, Opt. Lett. 16 (1991) 1168.
[14] G. Matthaus, J. Burghoff, M. Will, S. Nolte, A. Tunnermann, Appl. Phys. A 83 (2006) 347.
[15] Y. Sikorski, A.A. Said, P. Bado, R. Maynard, C. Florea, K.A. Winick, Electron. Lett. 36 (2000) 226.
[16] T. Ohtsuki, S. Honkanen, N. Peyghambarian, M. Takahashi, Y. Kawamoto, J. Ingenhoff, A. Tervonen, K. Kadono, Appl. Phys. Lett. 69 (1996) 2012.
[17] A. Peled, Ph.D. Thesis, Tel-Aviv University, in press.
[18] R.R. Goncalves, G. Carturan, L. Zampedri, M. Ferrari, M. Montagna, A. Chiasera, G.C. Righini, S. Pelli, S.J.L. Ribeiro, Y. Messaddeq, Appl. Phys. Lett. 81 (1) (2002) 28.
[19] A. Chiasera, M. Ferrari, L. Zampedri, M. Mattarelli, M. Montagna, H. Portales, C. Tosello, S. Dire, S. Pelli, G.C. Righini, Proc. SPIE 5451 (1) (2004) 574.
[20] L. Zampedri, M. Mattarelli, M. Montagna, R.R. Goncalves, Phys. Rev. B 75 (7) (2007) 73105.
[21] R.R. Goncalves, G. Carturan, M. Montagna, M. Ferrari, L. Zampedri, S. Pelli, G.C. Righini, S.J.L. Ribeiro, Y. Messaddeq, Opt. Mater. 25 (2) (2004) 131.
[22] N.D. Afify, R. Grisenti, G. Dalba, C. Armellini, M. Ferrari, S. Larcheri, F. Rocca, A. Kuzmin, Opt. Mater. 28 (6-7) (2006) 864.